Comparison of aerodynamic models for Vertical Axis Wind Turbines

Comparison of aerodynamic models for Vertical Axis Wind Turbines

C Simão Ferreira[1] and H Aagaard Madsen[2] and M Barone[3] and B Roscher[4] and P Deglaire[5] and I Arduin[5]

[1] Delft University of Technology - DUWIND, Delft, The Netherlands
[2] DTU Wind, Technical University of Denmark, Roskilde, Denmark
[3] Sandia National Laboratories, Albuquerque, New Mexico, United States of America
[4] Delft University of Technology & DTU Wind - European Wind Energy Master
[5] Areva Renewables, Paris, France

E-mail: c.j.simaoferreira@tudelft.nl, hama@dtu.dk, mbarone@sandia.gov, B.Roscher@student.tudelft.nl, paul.deglaire@areva.com, igor.arduin@areva.com

Abstract. Multi-megawatt Vertical Axis Wind Turbines (VAWTs) are experiencing an increased interest for floating offshore applications. However, VAWT development is hindered by the lack of fast, accurate and validated simulation models. This work compares six different numerical models for VAWTS: a multiple streamtube model, a double-multiple streamtube model, the actuator cylinder model, a 2D potential flow panel model, a 3D unsteady lifting line model, and a 2D conformal mapping unsteady vortex model. The comparison covers rotor configurations with two NACA0015 blades, for several tip speed ratios, rotor solidity and fixed pitch angle, included heavily loaded rotors, in inviscid flow. The results show that the streamtube models are inaccurate, and that correct predictions of rotor power and rotor thrust are an effect of error cancellation which only occurs at specific configurations. The other four models, which explicitly model the wake as a system of vorticity, show mostly differences due to the instantaneous or time averaged formulation of the loading and flow, for which further research is needed.

1. Introduction

The development of aerodynamic models for Vertical Axis Wind Turbines (VAWTs) has been hindered by the inherent complexity of the flow, and by an intermittent research effort which did not allow for an effective verification and validation [Sutherland et al., 2012]. Previous studies on VAWT model comparison are limited (e.g. [Wilson and McKie, 1978, Wilson and McKie, 1980, Simão Ferreira and Scheurich, 2013, Simão Ferreira, 2009]), with most work focusing on validation with experimental results (see [Paraschivoiu, 2002]).

In this work, we present a blind comparison of six models which use different formulations of the actuator and the wake/induction system. The six models are: the Multiple Streamtube Model (MST), the Double-Multiple Streamtube Model (DMST), the Actuator Cylinder model (AC), the U2DiVA code, the ARDEMA2D code, and the CACTUS code.

[3] Sandia National Laboratories is a multi-program laboratory managed and operated by Sandia Corporation, a wholly owned subsidiary of Lockheed Martin Corporation, for the U.S. Department of Energy's National Nuclear Security Administration under contract DE-AC04-94AL85000.

Table 1: Test cases.

Case	λ	σ	φ	Evaluated
A	2.5 : 0.5 : 7	0.04 : 0.005 : 0.14	0°	C_P, C_T
B	4.5	0.1, 0.14	0°	a, $a_\perp$, α, F_{tan}, F_{norm}, F_{st}
C	4.5	0.1	-3°, 0°, $+3^\circ$	a, $a_\perp$, α, F_{tan}, F_{norm}, F_{st}

The test cases are designed to distinguish between the integral (rotor average) and instantaneous (azimuthal distribution) results, identifying possible error cancellation. Rotor configuration is varied to test the range of validity of the models. To ensure the models are performing in the most similar conditions, the flow is assumed potential and the steady Bernoulli equation for pressure is used. Three main questions drive the research: 1) is the integral rotor performance (thrust and power) a suitable validation metric?; 2) can the models accurately predict the relation between actuator load and induction?; 3)what is the range of applicability of each model in terms of rotor loading and tip speed ratio?.

Section 2 presents the methods, test cases, and models; Section 3 presents the results of the test cases and their discussion and Section 4 presents the conclusions.

2. Methods

The six models are compared in simulations of a set of 2D test cases, for different tip speed ratios, rotor solidity and blade pitch, assuming inviscid flow. The compared values include: rotor power and thrust and the azimuthal distributions of induction (in wind and crosswind direction), perceived angle of attack, and normal, tangential and streamwise loads.

Section 2.1 describes the test cases; Section 2.2 defines the airfoil model of the NACA 0015, applied in the models that use an actuator point; and Section 2.3 describes the six models used.

2.1. Test cases

Table 1 lists the test cases. The rotor has two NACA 0015 profile blades. Three parameters are varied in each of the test cases: the rotor solidity $\sigma = \frac{B \cdot c}{2R}$, where B is the number of blades, c is the blade chord and R is the rotor radius; the tip speed ratio $\lambda = \frac{\Omega R}{U_\infty}$, where Ω is the rotational speed and U_∞ is the unperturbed wind speed; and the blade fixed pitch angle φ, with attachment point at the quarter-chord. Test case A aims to evaluate the effect of tip speed ratio and solidity on the power coefficient $C_P = \frac{Power}{0.5\rho 2RU_\infty^3}$ and rotor thrust coefficient $C_T = \frac{Thrust}{0.5\rho 2RU_\infty^2}$, where ρ if the fluid density. Test case B compares the azimuthal distributions of $a = 1 - u/U_\infty$ (windward induction factor), $a_\perp$ (crosswind induction factor), α (angle of attack), F_{tan} (tangential force), F_{norm} (radial force), F_{st} (force in wind direction). Case C tests the effect of changing the fixed pitch angle, with $(\sigma, \lambda, \varphi) = (0.1, 4.5, +3^\circ)$.

2.2. NACA 0015 airfoil

The NACA 0015 airfoil is used in both blades of all rotor configurations. The NACA 0015 is used in its inviscid flow formulation; the polars is defined by Equation 1.

$$c_l = 2\pi \cdot 1.11 \cdot \sin(\alpha) \text{ and } \mathrm{c_d} \quad = 0 \tag{1}$$

2.3. Description of the models

2.3.1. Multiple Streamtube model - MST In a blade element momentum model (BEM), the streamtube models determine the induced velocity in wind direction by equating the time-averaged load on the blades with the mean momentum flux (see [Wilson, 1980,

Wilson and Lissaman, 1974]). Three types of streamtube models are commonly used: single [Templin, 1974], multiple ([Wilson and Lissaman, 1974, Strickland, 1975]) and double-multiple ([Paraschivoiu, 2002]).

The Multiple Streamtube Model (MST) discretizes the crosswind direction into multiple adjacent streamtubes, assuming streamtube independence in crosswind direction (see [Lissaman, 1976]), but considering a single induction value per streamtube, used for both the upwind and the downwind segments of the actuator.

The relation between thrust coefficient C_t and the induction factor a is given by Equation 2 (adapted from [Burton et al., 2001]).

$$C_t(a) = \begin{cases} 4a\,(1-a) & : -\infty < a \leq 1 - 0.5\sqrt{1.6} \\ 1.6 - 4\left(\sqrt{1.6} - 1\right)(1-a) & : a > 1 - 0.5\sqrt{1.6} \end{cases} \quad (2)$$

2.3.2. Double Multiple Streamtube model - DMST In the Double Multiple Streamtube model (DMST), the upwind and downwind regions are modelled as two actuators operating in tandem (see [Lapin, 1975]). The downwind half of the rotor is assumed to be in the fully expanded wake of the upwind half, such that $U_{\infty_d} = U_\infty\,(1 - 2a_u)$. The model neglects the effect of the downwind half of the rotor on the upwind half.

2.3.3. Actuator Cylinder model - AC The Actuator Cylinder (AC) is a steady Eulerian model developed by [Madsen, 1982, Madsen, 1983] and recently implemented in the aeroelastic code HAWC2 ([Madsen et al., 2013, Larsen, 2009]). The model extends the actuator Disc concept to an actuator surface coinciding with the swept area of the 2D VAWT, in which the reaction of the blade forces are applied as body forces (the 3D general model is described in [Madsen, 1988]).

2.3.4. U2DiVA The Unsteady Two-Dimensional Vorticity Aerodynamics model (U2DiVA) is a 2D unsteady multibody free-wake panel-code (see [Simão Ferreira, 2009]), following the formulation of [Katz and Plotkin, 2000]. The code models the bodies using a distribution of constant strength sources and doublets. The near wake is modelled as constant strength doublet panels, while the far wake is modelled with vortex points.

2.3.5. ARDEMA2D The ARDEMA2D code has been developed by AREVA based on the theory elaborated in the PhD research of [Deglaire, 2010] (see also [Deglaire et al., 2009, Österberg, 2010]). The code uses a conformal mapping approach to generate N arbitrary profiles. The wake is modelled as a free vortex particle wake; at each time step, a new wake element is shed, and the motion of the wake is determined by the influence of all flow elements and airfoils.

2.3.6. CACTUS code The Code for Axial and Cross-flow TUrbine Simulation (CACTUS) [Murray and Barone, 2011] is a three-dimensional free vortex code in which the rotor blades are modelled using the lifting line approximation, with each blade discretized into a number of blade elements containing a bound vortex line. The wake is represented using a free vortex lattice; at each time step, each blade element produces a new shed vortex line segment connected to the bound vortex by two trailing vortex line segments. The velocity field induced by the entire vortex system, including bound and wake vortex elements, is calculated using the Biot-Savart law. The bound vortex strengths are calculated by determining the blade element force consistent with the local flow at each element produced by the wake, free-stream velocity, and the bound vorticity.

3. Results and discussion

3.1. Results and discussion for test case A

Figure 1 shows the power coefficient (C_P) and thrust coefficient (C_T) for tip speed ratios $2.5 \geq \lambda \geq 7$ and rotor solidity $0.04 \geq \sigma \geq 0.14$. The results are obtained from simulations with all models except the ARDEMA2D. The grey region of the DMST results is defined by the occurrence of flow reversal at the rotor ($a_u > 0.5$), for which the model is invalid. For the CACTUS code, the results correspond only to the mid-plane of the rotor, approximating a 2D flow. The results shows significant differences between the models. All models show iso-curves along lines defined by $\lambda\sigma = N_1$ where N_1 is an arbitrary constant. This result is expected since the term $\lambda\sigma$ is associated with actuator loading. However, there is a noticeable difference between the models that assume a time average loading on the actuator and time averaged solution of the induction/wake (MST, DMST and Actuator Cylinder) and the models that use an unsteady and instantaneous formulation of the loads, wake and induction (U2DiVA and CACTUS). For the former, C_P and C_T are constant along $\lambda\sigma = N_1$; for the latter models, there is an effect of the finite number of blades, where the peak C_P is found close to the lower solidity and higher tip speed ratio, as the solution tends to approximate an infinite number of blades rotating infinitely fast. The inclusion of a sub model in the actuator models for the shed voricity effect would probably yield a solution closer to the instantaneous models.

The DMST model is clearly limited in terms of the maximum loading. It is interesting to see that, for regions of high $\lambda\sigma$ for which the model is theoretically still valid (e.g. $(\lambda\sigma) = (5.5, 0.1)$), the results for C_T for the DMST model significantly differ from those of the other models, although the results of C_P are still close to those of the other models. This is an example of error cancellation that is demonstrated in the test cases B and C.

The Actuator Cylinder model shows increasing C_P with increasing C_T, while the other models show a decreasing C_P with increasing C_T after the maximum C_P. The reason for this behaviour is probably that the correction method of the linear solution becomes less accurate at the very high loading [Madsen et al., 2013].

3.2. Results and discussion for test case B

Figures 2 and 3 show the azimuthal distributions of a, $a_\perp$, α, F_{tan}, F_{norm}, F_{st} for, respectively, $(\sigma, \lambda, \varphi) = (0.1, 4.5, 0°)$ and $(0.14, 4.5, 0°)$, calculated with the six models.

Test case B shows that the MST model is not able to approximate the azimuthal distribution predicted by the other models in any of the configurations. The results show that the reasonable results of C_P and C_T in test case A are actually the result of the cancellation of the error in the prediction in loading between the upwind and downwind halves of the rotor.

The DMST appears to have a slightly better performance in the lighter loaded case ($(\lambda\sigma) = (4.5, 0.1)$, but shows very large differences to the other models for more heavier loaded case, even in the upwind half of the rotor. Because the DMST assumes $a_\perp = 0$, its results in the leeward and windward regions of the rotor are in disagreement with the vorticity based models. The assumption of full wake expansion of the streamtube between the upwind and downwind regions is incorrect, as shown by the comparison with the other models.

For the four models that explicitly model the vorticity field, there appears to be a difference between the Actuator Cylinder, that uses a time averaged loading on the actuator, and the U2DiVA, ARDEMA2D and CACTUS models, which consider the instantaneous loads. These differences are most noticeable in the estimation of a and $a_\perp$, especially in the leeward and windward regions of the rotor.

3.3. Results and discussion for test case C

Figure 4 shows the results of test case C for $\varphi = +3°$, $\lambda = 4.5$ and $\sigma = 0.1$, namely a, $a_\perp$, α, F_{norm}, F_{tan} and F_{st}. Table 2 present the results for test case C for C_T and C_P . The first

Table 2: C_T and C_P results from test case C. The first six columns contain the values for $\varphi = -3°$, $0°$ and $+3°$; the last four columns present the values for $\varphi = -3°$ and $+3°$ relative to the case $\varphi = 0°$.

	C_T			C_P			$C_T/C_{T_{\varphi=0°}}$		$C_P/C_{P_{\varphi=0°}}$	
	$-3°$	$0°$	$+3°$	$-3°$	$0°$	$+3°$	$-3°$	$+3°$	$-3°$	$+3°$
MST	0.92	0.92	0.92	0.55	0.55	0.55	1.00	1.00	1.00	1.00
DMST	1.02	0.87	0.63	0.70	0.60	0.50	1.17	0.73	1.18	0.84
Actuator Cylinder	0.90	0.89	0.89	0.59	0.59	0.60	1.00	1.00	0.99	1.02
U2DiVA	0.87	0.89	0.90	0.55	0.56	0.57	0.98	1.02	0.98	1.01
CACTUS	0.86	0.86	0.87	0.58	0.57	0.56	1.00	1.02	1.01	0.98
ARDEMA2D	0.90	0.92	0.94	0.61	0.63	0.65	0.98	1.02	0.97	1.03

six columns contain the values for $\varphi = -3°$, $0°$ and $+3°$; for easier comparison, the last four columns present the values for $\varphi = -3°$ and $+3°$ relative to the case $\varphi = 0°$.

Figures 2a and 4a show that, except for the DMST model, the induction a and $a_\perp$ almost does not change with the change of pitch angle. The change of pitch angle does cause a transfer of loading between upwind and downwind halves of the rotor, as seen in the radial force in Figures 2d and 4d, in the tangential force in Figures 2e and 4e, and in the streamwise force Figures 2f and 4f. The results in Table 2 show that for all models except the DMST model, the change of fixed pitch angle does not affect total power and thrust. Because the DMST model separates the two halves of actuator, it cannot model a zero net effect of adding a constant force, as is theoretically expected and verified by the other models. This result demonstrates a fundamental flaw of the DMST. A possible correction of the DMST model would then rely upon the subtraction of an average load to the upwind and downwind halves of the rotor; such approach has not yet been demonstrated.

4. Conclusions

The multiple streamtube model (MST) showed to deviate significantly from the other models, due to its simple induction model; it is however more internally consistent than the double multiple streamtube model (DMST), which proved to be fundamentally incorrect in the prediction of the effect of changing the fixed pitch angle. The results show that the agreement between DMST model results and the results of the other models occurs at a single configuration of solidity and tip speed ratio; therefore, power and thrust are insufficient validation parameters. In opposition to the conclusions by [Wilson and McKie, 1980], the results show that these models should be discontinued unless empirically corrected.

The results showed a good agreement between the models where the wake is explicitly modelled (Actuator Cylinder, U2DiVA, CACTUS and ARDEMA2D). The results point to the need to further investigate the effect of the near wake for instantaneous induction, in order to understand the differences between the time averaged approach and the unsteady approach. These models proved to be consistent with theory in relation to the effect of changing the fixed pitch angle. Future research will investigate the behaviour of these models in gusts and the impact of the error in the estimation of the fatigue life. Additionally, the models showed differences in the estimates of angle of attack that could have a significant impact in viscous simulations; this shows that the level of uncertainty of these models might still be too high for design purposes.

5. Acknowledgements

This work is made possible in part due to funds from the Dutch Technology Foundation STW - Veni grant, U.S DoE - Innovative Offshore Vertical-Axis Wind Turbine Rotor project, the

Future Emerging Technologies FP7 - Deepwind project, and AREVA.

References

[Burton et al., 2001] Burton, T., Sharpe, D., Jenkins, N., and Bossanyi, E. (2001). *Wind Energy Handbook*. John Wiley and Sons.

[Deglaire, 2010] Deglaire, P. (2010). *Analytical Aerodynamic Simulation Tools for Vertical Axis Wind Turbines*. PhD thesis, Uppsala University, Electricity. Felaktigt tryckt som Digital Comprehensive Summaries of Uppsala Dissertations from the Faculty of Science and Technology 704.

[Deglaire et al., 2009] Deglaire, P., Engblom, S., Ågren, O., and Bernhoff, H. (2009). Analytical solutions for a single blade in vertical axis turbine motion in two-dimensions. *European Journal of Mechanics-B/Fluids*, 28(4):506–520.

[Katz and Plotkin, 2000] Katz, J. and Plotkin, A. (2000). *Low-Speed Aerodynamics - 2nd Edition*. Cambridge Aerospace Series (No. 13). Cambridge University Press.

[Lapin, 1975] Lapin, E. (1975). Theoretical performance of vertical axis wind turbines. In *American Society of Mechanical Engineers, Winter Annual Meeting*, Houston, Texas.

[Larsen, 2009] Larsen, T. J. (2009). *How 2 Hawc2, the User's Manual*. Risø DTU, Roskilde, Denmark.

[Lissaman, 1976] Lissaman, P. B. S. (1976). Some marketing and technical considerations of wind power. In Ljungstrom, O., editor, *Advanced Wind Energy Systems*, volume 1, pages 2–37.

[Madsen, 1988] Madsen, H. (1988). Application of actuator surface theory on wind turbines. In *IEA meeting on Joint Actions on Aerodynamics of Wind Turbines, 2. Symposium*, Lyngby. Department of Fluid Mechanics, Technical University of Denmark.

[Madsen et al., 2013] Madsen, H., Larsen, T., Vita, L., and Paulsen, U. (2013). Implementation of the actuator cylinder flow model in the HAWC2 code for aeroelastic simulations on vertical axis wind turbines. In *51st AIAA Aerospace Sciences Meeting including the New Horizons Forum and Aerospace Exposition*.

[Madsen, 1982] Madsen, H. A. (1982). The actuator cylinder - a flow model for vertical axis wind turbines. Technical report, Institute of Industrial Constructions and Energy Technology - Aalborg University Centre.

[Madsen, 1983] Madsen, H. A. (1983). On the ideal and real energy conversion in a straight bladed vertical axis wind turbine. Technical report, Institute of Industrial Constructions and Energy Technology - Aalborg University Centre.

[Murray and Barone, 2011] Murray, J. C. and Barone, M. (2011). The development of CACTUS: a wind and marine turbine performance simulation code. AIAA 2011-147, 49th AIAA Aerospace Sciences Meeting, Orlando, FL.

[Österberg, 2010] Österberg, D. (2010). Multi-body unsteady aerodynamics in 2D applied to a Vertical-Axis Wind Turbine using a vortex method.

[Paraschivoiu, 2002] Paraschivoiu, I. (2002). *Wind turbine design with emphasis on Darrieus Concept*. Polytechnic International Press.

[Simão Ferreira, 2009] Simão Ferreira, C. (2009). *The near wake of the VAWT: 2D and 3D views of the VAWT aerodynamics*. PhD thesis, Delft University of Technology. ISBN/EAN:978-90-76468-14-3.

[Simão Ferreira and Scheurich, 2013] Simão Ferreira, C. and Scheurich, F. (2013). Demonstrating that power and instantaneous loads are decoupled in a vertical axis wind turbine. *Wind Energy*. Accepted For Publication.

[Strickland, 1975] Strickland, J. (1975). The Darrieus turbine - a performance prediction model using multiple streamtube. Technical Report SAND75-0431, Sandia National Laboratories.

[Sutherland et al., 2012] Sutherland, H. J., Berg, D. E., and Ashwill, T. D. (2012). A retrospective of VAWT technology. Technical Report SAND2012-0304, Sandia National Laboratories.

[Templin, 1974] Templin, R. (1974). Aerodynamic performance theory of the NRC vertical-axis wind turbine. Technical Report LTR-LA-160, National Research Council of canada.

[Wilson, 1980] Wilson, R. (1980). Wind-turbine aerodynamics. *Journal of Wind Engineering and Industrial Aerodynamics*, 5(3-4):357–372.

[Wilson and McKie, 1978] Wilson, R. and McKie, W. (1978). A comparison of aerodynamic analyses for the Darrieus rotor. In *Second International Symposium on Wind Energy Systems*, volume 2. BHRA fluid engineering and ECN - Netherlands Energy Research Foundation.

[Wilson and McKie, 1980] Wilson, R. and McKie, W. (1980). A comparison of aerodynamic analyses for the Darrieus rotor. In *Aerospace Sciences Meetings, Wind Energy Conference*, volume 2. American Institute of Aeronautics and Astronautics.

[Wilson and Lissaman, 1974] Wilson, R. E. and Lissaman, P. B. S. (1974). *Applied Aerodynamics of Wind Turbines*. Oregon State University.

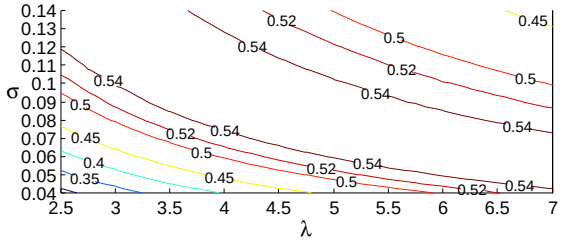

(a) C_P - MST.

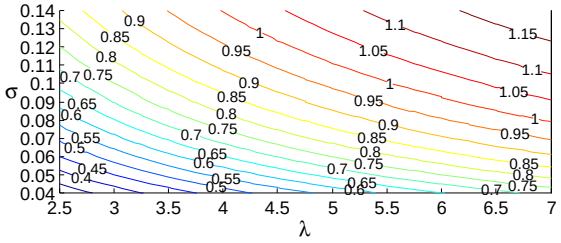

(b) C_T - MST.

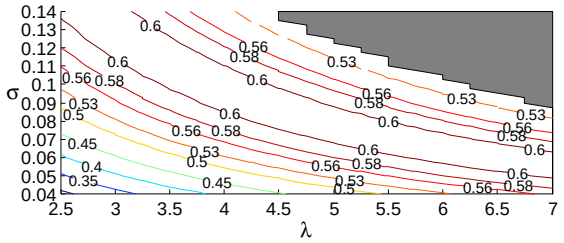

(c) C_P - DMST.

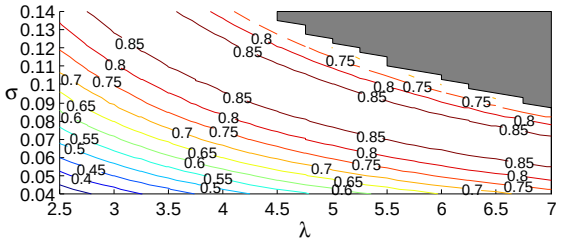

(d) C_T - DMST.

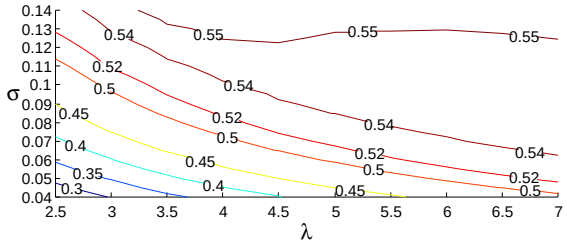

(e) C_P - Actuator Cylinder.

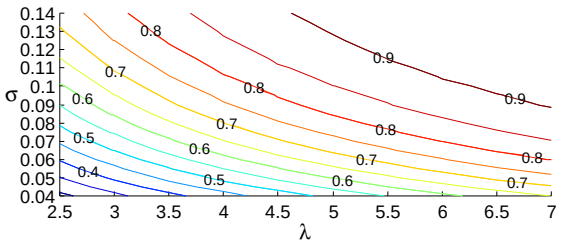

(f) C_T - Actuator Cylinder.

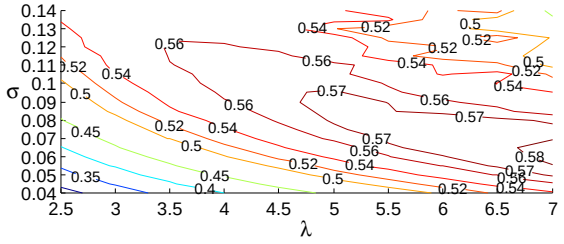

(g) C_P - U2DiVA.

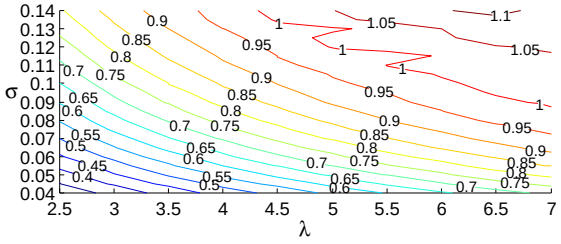

(h) C_T - U2DiVA.

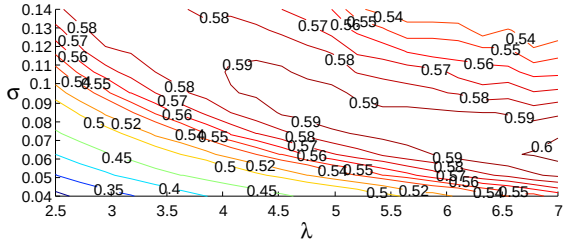

(i) C_P - CACTUS.

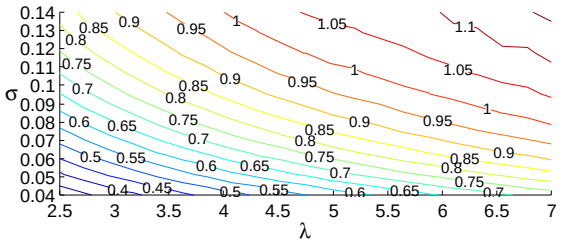

(j) C_T - CACTUS.

Figure 1: Results test case A. Power coefficient (C_P) and thrust coefficient (C_T) for tip speed ratios $2.5 \geq \lambda \geq 7$ and rotor solidity $0.04 \geq \sigma \geq 0.14$, with pitch angle $\psi = 0°$.

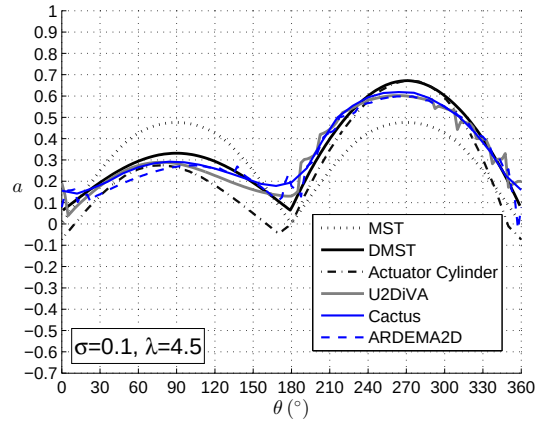

(a) a.

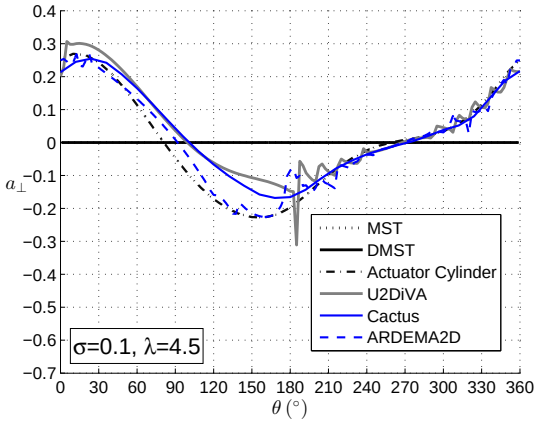

(b) $a_\perp$.

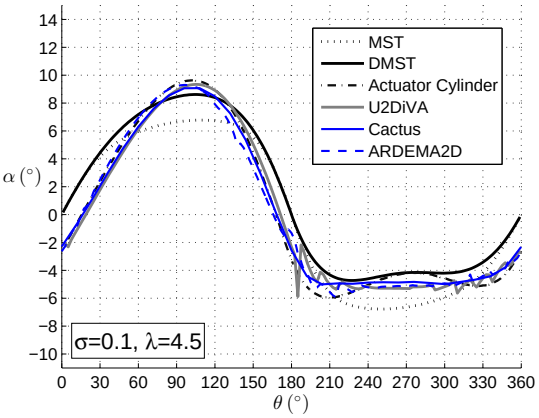

(c) α.

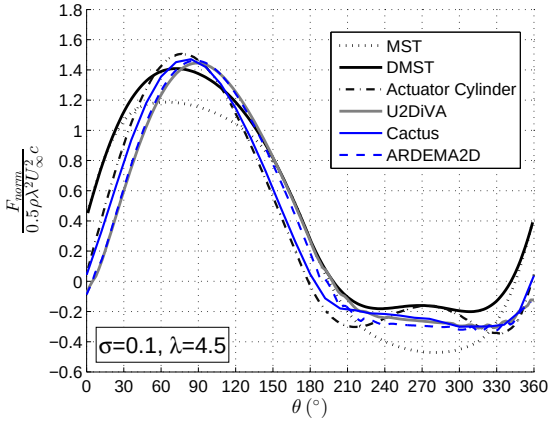

(d) F_{norm}.

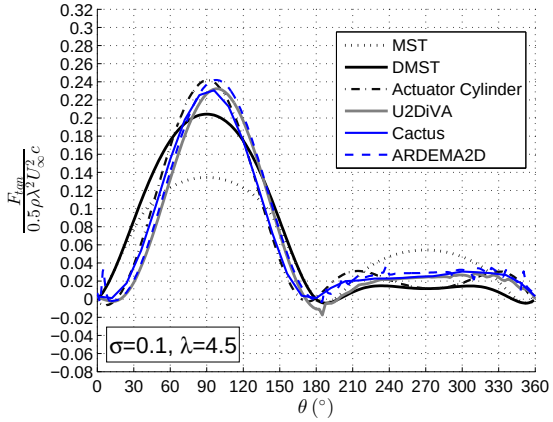

(e) F_{tan}.

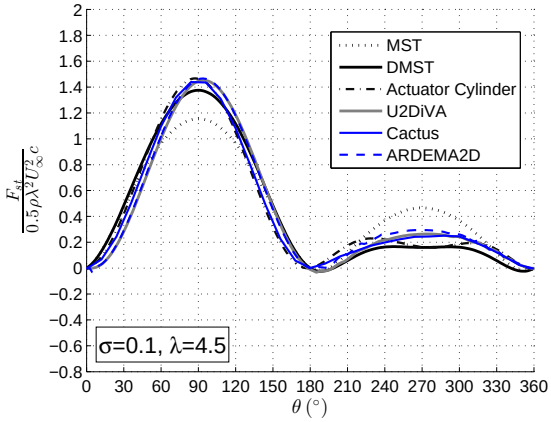

(f) F_{st}.

Figure 2: Results test case B, $\varphi = 0°$, $\lambda = 4.5$ and $\sigma = 0.1$. Induction factors a and $a_\perp$, angle of attack α and loading on blade in normal/radial direction F_{norm}, tangential/azimuthal direction F_{tan} and aligned with U_∞ (streamtube direction) F_{st}.

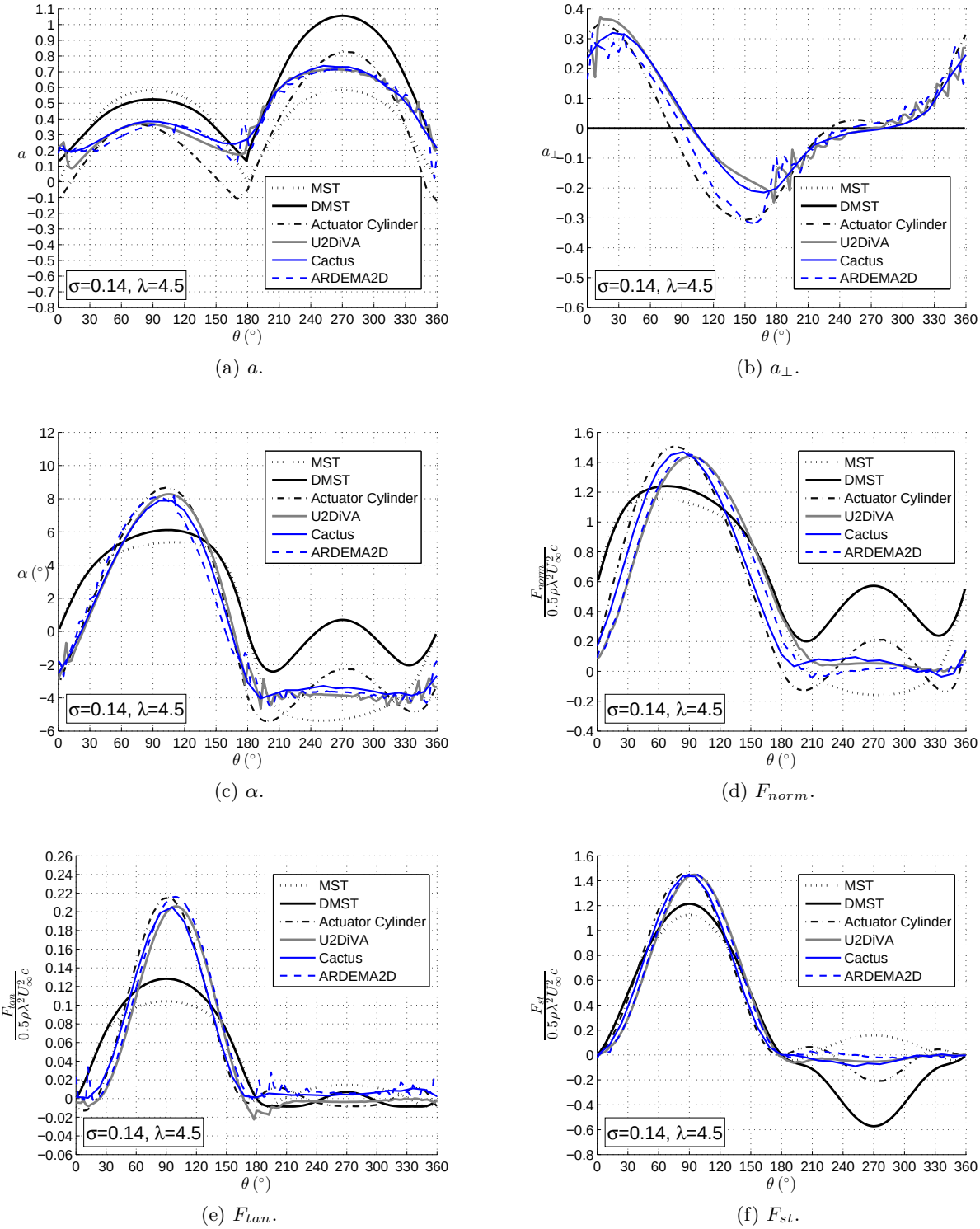

(a) a. (b) $a_\perp$.

(c) α. (d) F_{norm}.

(e) F_{tan}. (f) F_{st}.

Figure 3: Results test case B, $\varphi = 0°$, $\lambda = 4.5$ and $\sigma = 0.14$. Induction factors a and $a_\perp$, angle of attack α and loading on blade in normal/radial direction F_{norm}, tangential/azimuthal direction F_{tan} and aligned with U_∞ (streamtube direction) F_{st}.

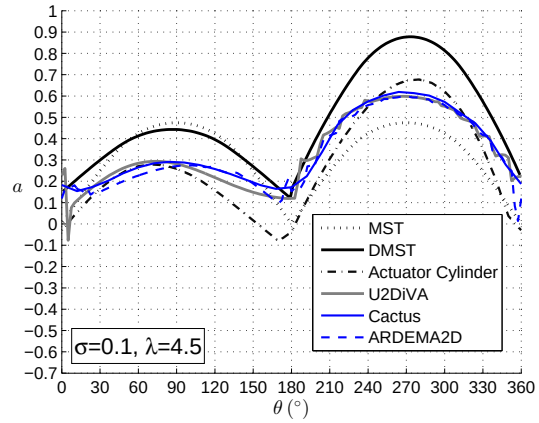

(a) a.

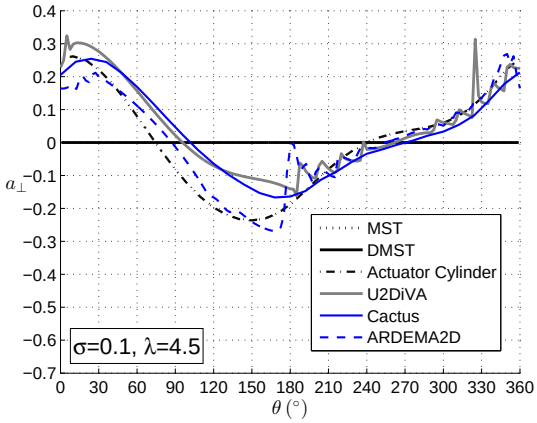

(b) $a_\perp$.

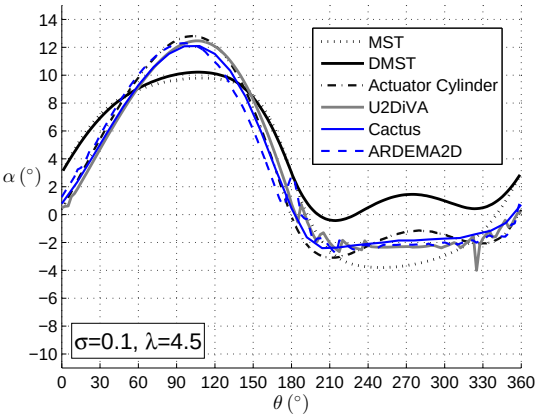

(c) α.

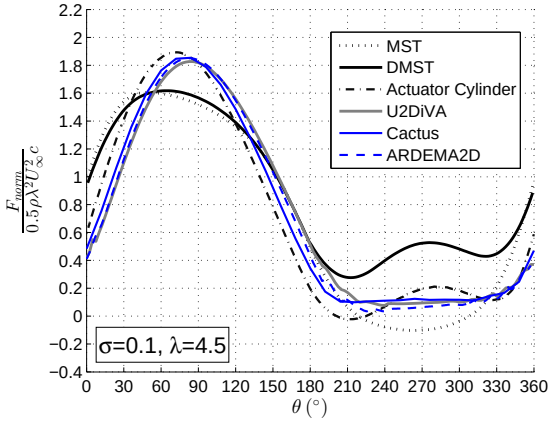

(d) F_{norm}.

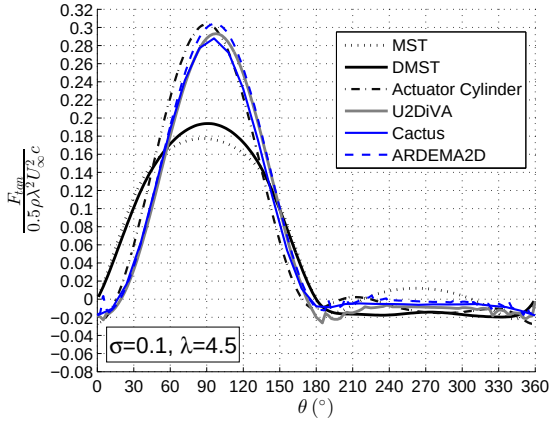

(e) F_{tan}.

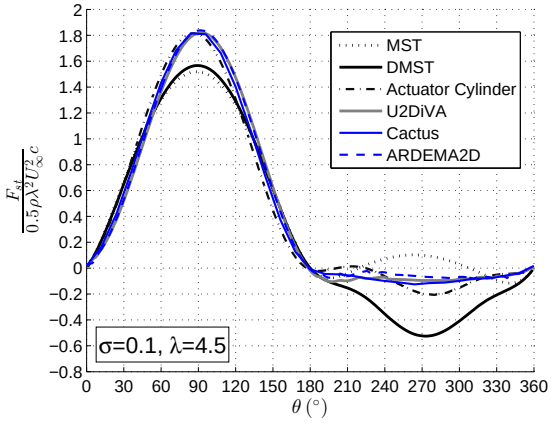

(f) F_{st}.

Figure 4: Results test case C, $\varphi = +3°$, $\lambda = 4.5$ and $\sigma = 0.1$. Induction factors a and $a_\perp$, angle of attack α and loading on blade in normal/radial direction F_{norm}, tangential/azimuthal direction F_{tan} and aligned with U_∞ (streamtube direction) F_{st}.